

# Fidelity and quantum geometry approach to Dirac exceptional points in diamond nitrogen-vacancy centers

Chia-Yi Ju,<sup>1,2</sup> Gunnar Möller,<sup>3,4</sup> and Yu-Chin Tzeng<sup>3,4,\*</sup>

<sup>1</sup>*Department of Physics and Center for Theoretical and Computational Physics,  
National Sun Yat-Sen University, Kaohsiung 80424, Taiwan*

<sup>2</sup>*Physics Division, National Center for Theoretical Sciences, Taipei 106319, Taiwan*

<sup>3</sup>*Physics of Quantum & Materials Group, School of Engineering,  
Mathematics and Physics, University of Kent, Canterbury CT2 7NH, United Kingdom*

<sup>4</sup>*Department of ElectroPhysics and Center for Theoretical and Computational Physics,  
National Yang Ming Chiao Tung University, Hsinchu 300093, Taiwan*

Dirac exceptional points (EPs) represent a novel class of non-Hermitian singularities that, unlike conventional EPs, reside entirely within the parity-time unbroken phase and exhibit linear energy dispersion. Here, we theoretically investigate the quantum geometry of Dirac EPs realized in nitrogen-vacancy centers in diamond, utilizing fidelity susceptibility as a probe. We demonstrate that despite the absence of a symmetry-breaking phase transition, the Dirac EP induces a pronounced geometric singularity, confirming the validity of fidelity in characterizing non-Hermitian EPs. Specifically, the real part of the fidelity susceptibility diverges to negative infinity, which serves as a signature of non-Hermitian criticality. Crucially, however, we reveal that this divergence exhibits a distinct anisotropy, diverging along the non-reciprocal coupling direction while remaining finite along the detuning axis. This behavior stands in stark contrast to the omnidirectional divergence observed in conventional EPs. Our findings provide a comprehensive picture of the fidelity probe near the Dirac EP, highlighting the critical role of parameter directionality in exploiting Dirac EPs for quantum control and sensing applications.

## I. INTRODUCTION

Non-Hermitian physics has emerged as a fertile ground for discovering exotic topological features and singularities that have no counterparts in Hermitian systems. At the heart of these unique phenomena lie the exceptional points (EPs), which represent singularities embedded in the system's parameter space where the Hamiltonian becomes mathematically defective. Distinct from conventional Hermitian degeneracies, an EP corresponds to a specific critical point in the parameter space where both eigenvalues and eigenstates coalesce, rendering the eigenbasis incomplete [1–4]. Beyond their fundamental theoretical intrigue [5–18], EPs have garnered significant attention for their functional utility in quantum technologies. The singular coalescence of eigenstates at the EP leads to a divergent response to external perturbations, a property that has been harnessed to significantly enhance the sensitivity of sensors [19–23], despite ongoing debate[24–33]. This extreme susceptibility renders non-Hermitian systems a promising platform for next-generation sensing devices, surpassing the fundamental limits of traditional Hermitian schemes.

While conventional EPs in parity-time symmetric systems [i.e., systems with parity-inversion (P) and time-reversal (T) symmetry] are typically associated with fractional power singularities and mark the boundary of PT symmetry breaking, a novel class of singularities, termed Dirac EPs, has recently been identified [34, 35]. Unlike

conventional EPs, the Dirac EP can exist entirely within the PT-unbroken phase, maintaining a purely real energy spectrum despite the non-Hermitian coalescence of eigenstates. This singularity draws a compelling analogy to the Dirac cones found in relativistic quantum mechanics and topological phases in Hermitian condensed matter physics, ranging from two-dimensional graphene [36–38] to three-dimensional Dirac and Weyl semimetals [39–47]. However, a fundamental difference lies in their realization: while these Hermitian Dirac cones reside in the physical momentum space governed by crystal symmetries, the non-Hermitian Dirac EP emerges in a synthetic parameter space. Here, tunable experimental parameters act as effective momenta, generating a linear dispersion relation and unique topological signatures independent of spatial translation symmetry. Following its initial proposal and demonstration in photonic systems [34], the Dirac EP was recently realized in a solid-state quantum system using a nitrogen-vacancy (NV) center in diamond [35], opening new avenues for exploring non-Hermitian topology in quantum sensing.

A comprehensive understanding of Dirac EPs demands that we look beyond the spectral degeneracy and examine the structure of the underlying parameter space. This geometry is naturally described by the quantum geometric tensor [48–53], whose real component defines the quantum metric of the manifold. In the context of quantum information, this metric is intimately related to the fidelity susceptibility [51], which characterizes the sensitivity of eigenstates to infinitesimal parameter perturbations. Previous theoretical frameworks have established geometric laws for conventional EPs associated with PT symmetry breaking. Specifically, analytical lemmas have

\* [yctzeng@nycu.edu.tw](mailto:yctzeng@nycu.edu.tw)

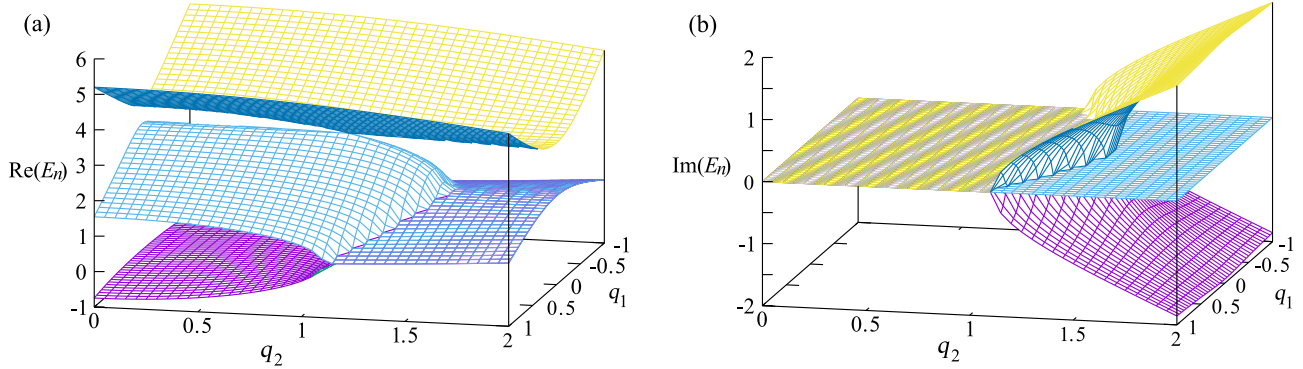


FIG. 1. The energy spectrum of the non-Hermitian Hamiltonian, Eq. (1). (a) The real part of the eigenenergies,  $\text{Re}(E_n)$ , revealing a Dirac cone structure centered at the Dirac EP  $(q_1, q_2) = (0, 1)$  within the PT-unbroken phase. (b) The imaginary part of the eigenenergies,  $\text{Im}(E_n)$ . The system remains in the PT-unbroken phase characterized by purely real eigenvalues for small  $q_2$ , but transitions to the PT-broken phase exhibiting non-zero imaginary components when the non-reciprocal coupling exceeds a critical threshold bounded by conventional EPs.

demonstrated that for a pair of states straddling a phase transition, where one state resides in the PT-unbroken phase and the other in the PT-broken phase, the real part of the fidelity approaches a fixed limit of  $1/2$  [52]. Furthermore, when approaching a conventional EP specifically from the PT-broken phase, the real part of the fidelity susceptibility has been shown to diverge to negative infinity [51, 52]. However, Dirac EPs present a fundamental challenge to these established results because they reside entirely within the PT-unbroken phase and do not demarcate a transition between broken and unbroken regimes. Consequently, the prerequisite conditions for the previous lemmas, namely either straddling the phase boundary or approaching from the broken phase, are absent. It is thus entirely unknown whether the fidelity approaching a Dirac EP retains any universal feature, or if the unique linear energy dispersion induces a novel geometric anisotropy that defies the behavior of conventional EPs.

In this work, we theoretically investigate fidelity-based geometric signatures of Dirac EPs within a physically realizable solid-state NV center platform. We first identify these signatures numerically through the fidelity susceptibility across the synthetic parameter space, and subsequently provide a physical interpretation rooted in the defective eigenstate structure of the Dirac EP. Our analysis focuses on an effective non-Hermitian Hamiltonian describing NV centers in diamond, a solid-state system in which Dirac EPs have been experimentally observed [35]. This platform therefore provides an ideal and experimentally relevant testbed for exploring the quantum geometry of Dirac EPs.

While theoretical frameworks such as the generalized vielbein formalism have been proposed to map non-Hermitian Hamiltonians onto Hermitian ones via metric deformations [54], the experimental realization considered here relies on the quantum dilation method [55, 56]. By coupling the spin-1 electronic qutrit to an ancillary nuclear spin, the composite system evolves under a di-

lated  $6 \times 6$  Hermitian Hamiltonian. Conditional measurements and post-selection on the ancilla state then project an effective  $3 \times 3$  non-Hermitian Hamiltonian, enabling precise engineering of the structure required to host Dirac EPs.

Leveraging this controllable platform, we calculate the fidelity susceptibility across the synthetic parameter space to characterize the geometric properties of the Dirac EP. We demonstrate that the Dirac EP indeed induces a geometric singularity, confirming the universality of fidelity as a probe even entirely within the PT-unbroken phase. Crucially, however, we reveal that this divergence exhibits a singular anisotropy: the susceptibility diverges to negative infinity along the coupling parameter direction while remaining finite along the detuning axis. This behavior stands in stark contrast to conventional EPs, where the geometric singularity is robust against the direction of approach. Our results thus provide a more comprehensive picture of fidelity-based detection, establishing its validity and unique signatures across the full spectrum of non-Hermitian singularities.

## II. MODEL AND METHOD

We consider a single nitrogen-vacancy center in diamond, which constitutes a spin-1 qutrit system. To explore the fidelity properties of Dirac EPs, we employ the effective non-Hermitian Hamiltonian experimentally realized via the quantum dilation method [35]. Originating from a truncated tight-binding model with non-reciprocal couplings, the effective Hamiltonian governing the system dynamics is given by:

$$H(q_1, q_2) = 3S_z^2 + 2q_1S_z + \sqrt{2}(S_x - iq_2S_y), \quad (1)$$

where  $S_{x,y,z}$  are the standard spin-1 operators. In this synthetic parameter space, the dimensionless parameters  $q_1$  and  $q_2$  correspond to the effective momentum

and the degree of non-reciprocal coupling, respectively. The interplay between the diagonal terms and the non-Hermitian coupling term  $\sqrt{2}(S_x - iq_2 S_y)$  generates the specific topological structure required to host the Dirac EP.

Given the non-Hermitian nature of the Hamiltonian where  $H \neq H^\dagger$ , the left  $|L_n\rangle$  and right  $|R_n\rangle$  eigenstates are distinct. These states are defined by the eigenvalue equations  $\langle L_n|H = E_n\langle L_n|$  and  $H|R_n\rangle = E_n|R_n\rangle$ , where the band index  $n$  takes values of 0 and  $\pm 1$ , with  $n = 0$  denoting the specific state under investigation. Away from the EPs, these eigenstates form a complete biorthogonal basis satisfying the normalization condition  $\langle L_n|R_m\rangle = \delta_{nm}$  and the completeness relation

$$\sum_n |R_n\rangle\langle L_n| = \mathbb{1}. \quad (2)$$

The resulting energy spectrum  $E_n(q_1, q_2)$  is illustrated in Fig. 1. A key feature of the Dirac EP is its location within the PT-unbroken phase. As shown in Fig. 1(a), the eigenvalues remain purely real in the vicinity of the Dirac EP at  $(q_1, q_2) = (0, 1)$ , where the bands exhibit a linear crossing characteristic of a Dirac cone. This stands in contrast to conventional EPs, which typically mark the boundary of PT-symmetry breaking. However, as the non-reciprocal coupling  $q_2$  increases beyond a critical threshold, the system eventually undergoes a transition to the PT-broken phase. As observed in Fig. 1(b), this transition is accompanied by the emergence of conventional EPs (square-root singularities) and complex conjugate eigenenergies. In this work, we focus primarily on the quantum geometry near the Dirac EP in the real-spectrum regime.

It is important to note that the completeness relation Eq. (2) holds strictly only when the Hamiltonian is diagonalizable. At the exact EP, the eigenstates coalesce, rendering the eigenbasis defective and the resolution of identity invalid. In such defective regimes, a more rigorous treatment involves introducing a metric operator to characterize the curved Hilbert space geometry [57–63]. However, the present study focuses on the quantum geometry within the PT-unbroken phase as the system approaches the EP. Since the system parameters remain in the non-defective regime where the spectrum is real and non-degenerate, the biorthogonal formalism remains rigorously well-defined and is consistent with the post-selection measurement scheme employed in experiments.

To elucidate the intrinsic geometry of the Dirac EP, we employ the fidelity susceptibility as a probe in the parameter space. While the definition of fidelity is not strictly unique even within Hermitian quantum mechanics [64–70], distinct formulations in the Hermitian context typically yield qualitatively consistent physical predictions regarding phase transitions. For non-Hermitian systems, however, the choice of definition warrants careful consideration because different generalizations can emphasize distinct facets of the underlying quantum geometry [48–52, 71–75]. In this study, we adopt the fidelity

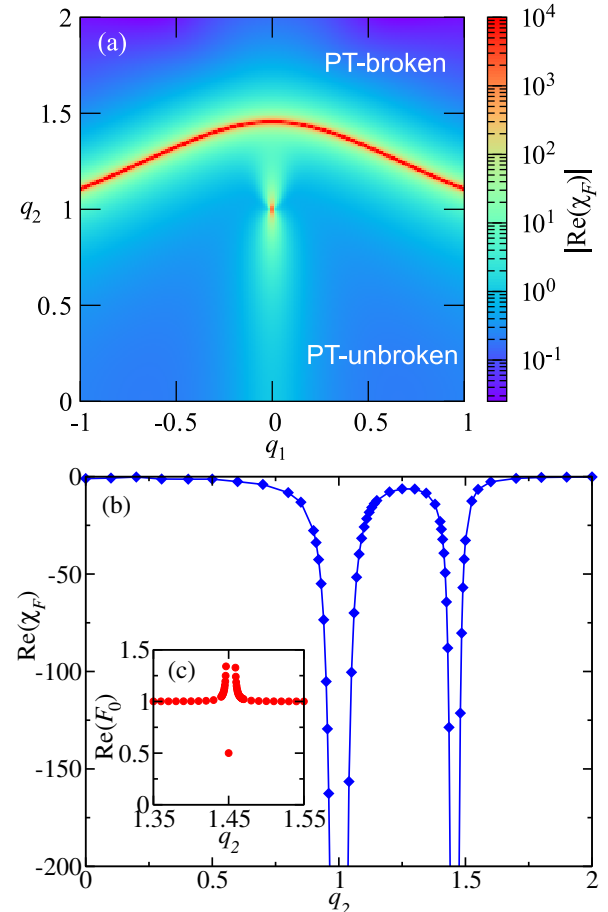


FIG. 2. (a) Density plot of the real part of the fidelity susceptibility  $|\text{Re}(\chi_F)|$  in the  $(q_1, q_2)$  plane. The red spot at  $(0, 1)$  corresponds to the Dirac EP, while the red curves indicate the exceptional lines formed by conventional EPs. (b) Behavior of  $\text{Re}(\chi_F)$  along the  $q_2$  axis with  $q_1 = 0$  fixed, demonstrating sharp divergences to negative infinity at both the Dirac EP and conventional EPs. (c) The real part of the fidelity  $F_0$  between states at  $q_2$  and  $q_2 + \delta q$  with fixed  $q_1 = 0$ . As the system straddles the conventional EP boundary,  $\text{Re}(F_0)$  approaches the universal limit of  $1/2$ .

defined as the complex-valued product of biorthogonal overlaps [51, 52]. This specific formulation is advantageous as it preserves the metric structure of the Hilbert space and exhibits robust universal properties [52, 60, 76]. Most notably, the real part of the fidelity susceptibility in this formalism diverges to negative infinity, which provides a sharp contrast to the positive infinity divergence characteristic of conventional Hermitian quantum phase transitions.

Specifically, for a multi-parameter Hamiltonian  $H(\vec{q})$  with  $\vec{q} = (q_1, q_2)$ , the fidelity between the states at  $\vec{q}$  and  $\vec{q} + \delta\vec{q} = \vec{q} + \delta q \hat{n}$  is defined and expanded as

$$F_n(\vec{q}, \vec{q} + \delta\vec{q}) = \langle L_n(\vec{q} + \delta\vec{q}) | R_n(\vec{q}) \rangle \langle L_n(\vec{q}) | R_n(\vec{q} + \delta\vec{q}) \rangle \quad (3)$$

$$= 1 - \chi_F^{(n)} \delta q^2 + \mathcal{O}(\delta q^3), \quad (4)$$

where  $\hat{n}$  is a unit vector in the parameter space specify-

ing the direction of displacement. The second-order coefficient  $\chi_n$  represents the leading non-trivial contribution to the fidelity expansion, defined as

$$\chi_F^{(n)}(\vec{q}, \hat{n}) = \lim_{\delta q \rightarrow 0} \frac{1 - F_n(\vec{q}, \vec{q} + \delta q \hat{n})}{\delta q^2}. \quad (5)$$

This formulation highlights that the fidelity susceptibility is inherently direction-dependent, allowing for a precise characterization of the directional sensitivity to parameter perturbations. Notably, within the PT-unbroken phase, the fidelity remains purely real [52], ensuring that  $\chi_F^{(n)}$  remains a real-valued measure throughout the regime where the energy spectrum is real. Hereafter we refer  $\chi_F^{(0)}$  to as  $\chi_F$ .

### III. NUMERICAL RESULTS

We proceed by analyzing the fidelity measure focusing on the middle  $n = 0$  band, and in what follows use the shorthand  $\chi_F \equiv \chi_F^{(0)}$  to describe our numerical results. Figure 2(a) provides a global view of the singular features in the parameter space by mapping the real part of the fidelity susceptibility for the  $n = 0$  state. Two distinct types of singularities are clearly visible: a localized singularity at  $(q_1, q_2) = (0, 1)$  identifying the Dirac EP and a continuous boundary of singularities corresponding to the exceptional line composed of conventional EPs. This landscape demonstrates that the fidelity susceptibility serves as a sensitive geometric probe, effectively capturing the distinct signatures of both the novel Dirac EP and the conventional EPs.

To quantitatively examine the divergent behavior, we investigate the parameter space along the  $q_2$  axis by setting  $q_1 = 0$  and choosing the displacement direction  $\hat{n} = (0, 1)$ , as depicted in Fig. 2(b). Along this trajectory,  $\text{Re}(\chi_0)$  exhibits sharp singularities, diverging to negative infinity as the system approaches both the Dirac EP and the conventional EPs. This observation confirms that the geometric signatures previously established for non-Hermitian degeneracies [51, 52] remain valid for Dirac EPs, indicating that the negative divergence of the fidelity susceptibility constitutes a robust and universal hallmark of non-Hermitian singularities.

We further examine the behavior near conventional EPs by considering parameter steps that straddle the exceptional boundary,  $q_2 < q_{\text{EP}} < q_2 + \delta q$ . As shown in Fig. 2(c), the real part of the fidelity  $\text{Re}(F_0)$  converges to the universal value of  $1/2$  predicted for transitions between PT-unbroken and PT-broken phases [52]. Together, these results validate fidelity susceptibility as a unified geometric probe capable of detecting both conventional and Dirac EPs.

Having established this universal behavior, we now turn to a key distinction that sets the Dirac EP apart from conventional EPs: its pronounced directional dependence. To further elucidate the intrinsic geometry of

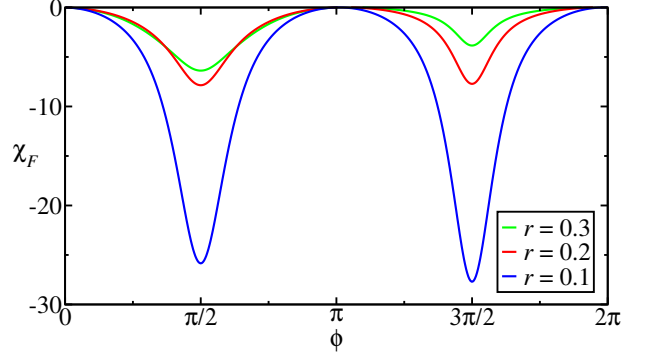


FIG. 3. The real part of the fidelity susceptibility,  $\text{Re}(\chi_0)$ , calculated along the radial direction as a function of the polar angle  $\phi$  surrounding the Dirac EP. The curves correspond to different radial distances  $r = 0.1, 0.2, 0.3$ . The susceptibility exhibits a strong anisotropic divergence, peaking at  $\phi = \pi/2$  and  $3\pi/2$  (approaching along the  $k_2$  axis) while vanishing within numerical precision at  $\phi = 0$  and  $\pi$  (approaching along the  $k_1$  axis). This behavior indicates that the leading-order geometric response near the Dirac EP is highly directional in parameter space.

the Dirac EP, we investigate the angular dependence of the fidelity susceptibility in the vicinity of the singularity, as shown in Fig. 3. We introduce a polar coordinate system centered at the Dirac EP, defined by  $q_1 = r \cos \phi$  and  $q_2 = 1 + r \sin \phi$ , where  $r$  denotes the radial distance and  $\phi$  the polar angle. We then compute  $\chi_0$  along the radial direction by evaluating the fidelity between states at  $r$  and  $r - \delta r$  for different values of  $\phi$ .

Figure 3 further reveals that the anisotropy of the fidelity susceptibility is not merely quantitative but qualitative: while  $\text{Re}(\chi_F)$  diverges strongly for approaches aligned with the  $k_2$  axis, it vanishes within numerical precision for approaches along the  $k_1$  axis ( $\phi = 0, \pi$ ). As we show below, for the specific Hamiltonian considered here, the symmetry of the perturbation enforces that the leading-order eigenstate deformation along the generalized Jordan direction vanishes for parameter variations aligned with the  $k_1$  axis. As a result, the radial fidelity susceptibility is numerically indistinguishable from zero along these directions, whereas it diverges along directions that couple strongly to the defective channel.

### IV. ANALYTIC INTERPRETATION: EIGENSTATE GEOMETRY NEAR THE DIRAC EXCEPTIONAL POINT

To elucidate the physical origin of the anisotropic fidelity susceptibility observed in Figs. 2 and 3, we now develop an analytic description of the eigenstate structure in the vicinity of the Dirac exceptional point. While the energy spectrum near the Dirac EP exhibits a linear dispersion reminiscent of Hermitian Dirac cones, the singular geometric response uncovered in Sec. III originates from the defective nature of the underlying eigenstates

rather than from spectral gap closing. The following analysis demonstrates how this defectiveness constrains the quantum geometry and leads to a highly directional critical response.

### A. Jordan structure at the Dirac exceptional point

At the Dirac EP located at  $(q_1, q_2) = (0, 1)$ , two eigenvalues of the non-Hermitian Hamiltonian coalesce at energy  $E = 3$ , and the Hamiltonian becomes non-diagonalizable. As a result, the EP is characterized by a rank-2 Jordan block rather than a complete set of eigenvectors. One may therefore introduce a right Jordan chain  $\{|\psi_0\rangle, |\chi\rangle\}$  defined by

$$(H - 3\mathbb{1})|\psi_0\rangle = 0, \quad (H - 3\mathbb{1})|\chi\rangle = |\psi_0\rangle, \quad (6)$$

together with the corresponding left Jordan chain  $\{|\phi_0\rangle, |\eta\rangle\}$  satisfying

$$\langle\phi_0|(H - 3\mathbb{1}) = 0, \quad \langle\eta|(H - 3\mathbb{1}) = \langle\phi_0|. \quad (7)$$

These vectors span the defective subspace associated with the Dirac EP. Away from the EP, where the Hamiltonian remains diagonalizable and the spectrum is real and non-degenerate, the Jordan vectors continuously evolve into the two EP-related eigenstates.

### B. Eigenstate expansion near the Dirac EP

We now consider a small displacement away from the Dirac EP in parameter space,

$$q_1 = r \cos \phi, \quad q_2 = 1 + r \sin \phi, \quad (8)$$

with  $r \ll 1$ . In contrast to conventional EPs, where eigenstates generally exhibit fractional-power (Puiseux) expansions in the vicinity of the degeneracy [3, 77], the Dirac EP admits a regular Taylor expansion along real parameter directions.

A key feature of the Dirac EP is the asymmetric response of the two coalescing eigenstates. One branch remains geometrically inert to linear order,

$$|\Psi_-(r, \phi)\rangle = |\psi_0\rangle + \mathcal{O}(r^2), \quad (9)$$

while the other branch acquires a linear admixture of the generalized Jordan vector,

$$|\Psi_+(r, \phi)\rangle = |\psi_0\rangle + r A(\phi) |\chi\rangle + \mathcal{O}(r^2). \quad (10)$$

Here, the scalar coefficient

$$A(\phi) = \langle\phi_0|\delta H(\phi)|\psi_0\rangle \quad (11)$$

encodes the projection of the perturbation  $\delta H = r(\cos \phi \partial_{q_1} H + \sin \phi \partial_{q_2} H)$  onto the defective direction in Hilbert space.

Importantly, this expansion reveals that all leading-order eigenstate deformation near the Dirac EP is confined to a single direction in Hilbert space, namely the generalized Jordan vector  $|\chi\rangle$ . The EP eigenvector  $|\psi_0\rangle$  itself remains unchanged to linear order.

### C. Origin of anisotropic fidelity susceptibility

This constrained eigenstate structure provides a direct explanation for the directional dependence of the fidelity susceptibility observed numerically. Since the biorthogonal fidelity probes the overlap between eigenstates at nearby points in parameter space, its leading nontrivial contribution depends on how strongly the eigenstate changes along the direction of displacement.

Using the expansion above, the fidelity susceptibility of the sensitive branch takes the schematic form

$$\chi_F(\mathbf{q}, \hat{\mathbf{n}}) \sim -\frac{|\partial_{\hat{\mathbf{n}}} A(\phi)|^2}{[E_+(r, \phi) - E_-(r, \phi)]^2} + \chi_F^{(\text{reg})}, \quad (12)$$

where  $\hat{\mathbf{n}}$  denotes the direction of parameter variation and  $\chi_F^{(\text{reg})}$  represents finite contributions arising from non-degenerate bands.

Because the eigenvalue splitting near the Dirac EP is linear and remains nonzero in all real directions, the divergence of the fidelity susceptibility is not driven by a vanishing energy gap. Instead, it is governed by the angular dependence of the coefficient  $A(\phi)$ , which determines how strongly a given parameter displacement couples to the defective eigenstate direction.

As a result, parameter-space directions that induce a strong projection onto  $|\chi\rangle$  give rise to a divergent fidelity susceptibility, while directions orthogonal to this defective channel lead to a strong suppression of the radial fidelity response. This mechanism accounts for the pronounced anisotropy observed in Fig. 3.

### D. Geometric interpretation and contrast with conventional exceptional points

The analysis above highlights a fundamental geometric distinction between Dirac EPs and conventional EPs. For conventional EPs associated with PT-symmetry breaking, the geometric singularity is effectively isotropic and closely tied to the square-root closing of the energy gap. In contrast, the Dirac EP resides entirely within the PT-unbroken phase and exhibits a form of geometric criticality without spectral instability, but displaying a strong directional dependence.

The anisotropic divergence of the fidelity susceptibility reflects the fact that the quantum geometry near the Dirac EP is effectively rank-one at leading order: a single generalized Jordan direction in Hilbert space governs the singular response. Parameter-space directions orthogonal to this channel do not induce a first-order eigenstate deformation, even though the underlying geometric structure remains finite and well defined.

This directional sensitivity constitutes a defining geometric signature of the Dirac EP and provides the analytic foundation for the numerical observations presented in Sec. III.

## V. CONCLUSIONS

We have investigated the intrinsic quantum geometry of the Dirac exceptional point within a solid-state NV center system. By employing the fidelity susceptibility defined as the complex-valued product of biorthogonal overlaps [51], which notably remains purely real within the PT-unbroken phase [52], we established a unified geometric characterization of this novel class of non-Hermitian singularities.

A central finding of this study is that the Dirac EP shares a universal geometric hallmark with conventional EPs, namely the divergence of the real part of the fidelity susceptibility to negative infinity. This result demonstrates that geometric criticality is a robust feature of non-Hermitian degeneracies and persists even in the absence of a PT-symmetry breaking transition. The consistency of our approach is further corroborated by the analysis of conventional EPs within the same system, where the real part of the fidelity converges to the universal limit of 1/2 when the parameter displacement straddles the exceptional line.

Beyond this universality, we uncovered a pronounced and distinctive geometric anisotropy that fundamentally differentiates Dirac EPs from their conventional counterparts. While conventional EPs typically exhibit a divergence of the fidelity susceptibility that is insensitive to the direction of approach, the Dirac EP displays a highly directional response. In particular, the fidelity susceptibility diverges to negative infinity along the non-reciprocal coupling axis  $k_2$ , while being strongly suppressed along the effective momentum direction  $k_1$ , vanishing within numerical precision in the present model. Importantly, this anisotropy does not originate from vanishing spectral gaps, as the energy dispersion near the Dirac EP remains linear and nonzero in all real directions. Instead, it reflects the underlying defective eigenstate structure of the Dirac EP, in which the leading-order deformation of the eigenstate is confined to a single generalized Jordan direction in Hilbert space.

These results establish a comprehensive geometric understanding of non-Hermitian Dirac EPs by shifting the analytical focus from spectral degeneracies to the structure of eigenstates in parameter space. As a fundamental probe of quantum geometry, the fidelity susceptibility provides a sensitive and experimentally relevant benchmark for quantifying eigenstate response near non-

Hermitian singularities. The strong directional dependence revealed in this work demonstrates that geometric criticality at Dirac EPs is governed by specific structural constraints rather than being a uniform property. Consequently, our findings offer clear guidelines for the controlled manipulation of Dirac EPs, indicating that parameter variations must be carefully aligned with the directions of maximal geometric sensitivity to achieve predictable and enhanced responses. More broadly, this work establishes fidelity-based diagnostics as a powerful framework for exploring anisotropic geometric singularities in a wide range of emerging non-Hermitian platforms and engineered quantum materials.

Finally, we note that the fidelity-based geometric diagnostics discussed here are, in principle, accessible in several experimental platforms that realize non-Hermitian Hamiltonians via conditional dynamics. In the NV-center implementation of Ref. 35, the effective non-Hermitian evolution is engineered through quantum dilation, enabling direct access to biorthogonal state overlaps via conditional measurements and post-selection. More generally, non-Hermitian dynamics realized through post-selected quantum trajectories, such as in Ref. 34, also provide access to pure conditional states, from which state overlaps and fidelity susceptibilities may be inferred through repeated state preparation and measurement. These considerations suggest that fidelity-based probes offer a broadly applicable route to experimentally exploring the intrinsic geometry of non-Hermitian singularities.

## ACKNOWLEDGMENTS

CYJ and YCT are grateful for the support of the National Science and Technology Council (NSTC) of Taiwan under grant No. NSTC 112-2112-M-110-013-MY3 and 113-2112-M-A49-015-MY3, respectively. We thank the National Center for High-performance Computing (NCHC) of National Applied Research Laboratories (NARLabs) in Taiwan for providing computational and storage resources. This work is funded in part by a QuantEmX grant from ICAM and the Gordon and Betty Moore Foundation through Grant GBMF9616 to Gunnar Möller. GM also acknowledges the hospitality of the National Centre for Theoretical Sciences, Taiwan.

---

[1] C. M. Bender and S. Boettcher, Real spectra in non-Hermitian Hamiltonians having  $\mathcal{PT}$  symmetry, *Phys. Rev. Lett.* **80**, 5243 (1998).

[2] W. D. Heiss, Exceptional points of non-Hermitian operators, *J. Phys. A: Math. Gen.* **37**, 2455 (2004).

[3] W. D. Heiss, The physics of exceptional points, *J. Phys. A: Math. Theor.* **45**, 444016 (2012).

[4] M.-A. Miri and A. Alù, Exceptional points in optics and photonics, *Science* **363**, eaar7709 (2019).

[5] V. M. Martinez Alvarez, J. E. Barrios Vargas, and L. E. F. Foa Torres, Non-Hermitian robust edge states in one dimension: Anomalous localization and eigenspace condensation at exceptional points, *Phys. Rev. B* **97**, 121401 (2018).

[6] S. Longhi, Loschmidt echo and fidelity decay near an exceptional point, *Annalen der Physik*, 1900054 (2019).

[7] J.-C. Tang, S.-P. Kou, and G. Sun, Dynamical scaling of Loschmidt echo in non-Hermitian systems, *Europhysics Letters* **137**, 40001 (2022).

[8] L. E. F. Foa Torres, Perspective on topological states of non-Hermitian lattices, *J. Phys.: Materials* **3**, 014002 (2019).

[9] P.-Y. Chang, J.-S. You, X. Wen, and S. Ryu, Entanglement spectrum and entropy in topological non-Hermitian systems and nonunitary conformal field theory, *Phys. Rev. Research* **2**, 033069 (2020).

[10] Z. Yang, A. P. Schnyder, J. Hu, and C.-K. Chiu, Fermion doubling theorems in two-dimensional non-Hermitian systems for Fermi points and exceptional points, *Phys. Rev. Lett.* **126**, 086401 (2021).

[11] Y.-T. Tu, Y.-C. Tzeng, and P.-Y. Chang, Rényi entropies and negative central charges in non-Hermitian quantum systems, *SciPost Phys.* **12**, 194 (2022).

[12] M. Fossati, F. Ares, and P. Calabrese, Symmetry-resolved entanglement in critical non-Hermitian systems, *Phys. Rev. B* **107**, 205153 (2023).

[13] R. A. Henry and M. T. Batchelor, Exceptional points in the Baxter-Fendley free parafermion model, *SciPost Phys.* **15**, 016 (2023).

[14] P.-Y. Yang and Y.-C. Tzeng, Entanglement Hamiltonian and effective temperature of non-Hermitian quantum spin ladders, *SciPost Phys. Core* **7**, 074 (2024).

[15] D. Zou, T. Chen, H. Meng, Y. S. Ang, X. Zhang, and C. H. Lee, Experimental observation of exceptional bound states in a classical circuit network, *Science Bulletin* **69**, 2194 (2024).

[16] C.-Y. Ju, J. He, and G.-Y. Chen, Fractional exponents and topological signatures of exceptional points in non-Hermitian systems, *Ann. Phys.* **483**, 170270 (2025).

[17] Y. Zhou, W. Xia, L. Li, and W. Li, Diagnosing quantum many-body chaos in non-Hermitian quantum spin chain via Krylov complexity, *Phys. Rev. Res.* **7**, 033281 (2025).

[18] S. Longhi, Phase transitions and virtual exceptional points in quantum emitters coupled to dissipative baths, *J. Appl. Phys.* **138**, 184401 (2025).

[19] J. Wiersig, Enhancing the sensitivity of frequency and energy splitting detection by using exceptional points: Application to microcavity sensors for single-particle detection, *Phys. Rev. Lett.* **112**, 203901 (2014).

[20] H. Hodaei, A. U. Hassan, S. Wittek, H. Garcia-Gracia, R. El-Ganainy, D. N. Christodoulides, and M. Khajavikhan, Enhanced sensitivity at higher-order exceptional points, *Nature* **548**, 187 (2017).

[21] W. Chen, S. Kaya Özdemir, G. Zhao, J. Wiersig, and L. Yang, Exceptional points enhance sensing in an optical microcavity, *Nature* **548**, 192 (2017).

[22] H. Liu, D. Sun, C. Zhang, M. Groesbeck, R. McLaughlin, and Z. V. Vardeny, Observation of exceptional points in magnonic parity-time symmetry devices, *Science Advances* **5**, eaax9144 (2019).

[23] D.-Y. Chen, L. Dong, and Q.-A. Huang, A nonlinear parity-time-symmetric system for robust phase sensing, *Nat. Electron.* **10.1038/s41928-025-01542-8** (2026).

[24] W. Langbein, No exceptional precision of exceptional-point sensors, *Phys. Rev. A* **98**, 023805 (2018).

[25] H.-K. Lau and A. A. Clerk, Fundamental limits and non-reciprocal approaches in non-Hermitian quantum sensing, *Nat. Commun.* **9**, 4032 (2018).

[26] M. Zhang, W. Sweeney, C. W. Hsu, L. Yang, A. Stone, and L. Jiang, Quantum noise theory of exceptional point amplifying sensors, *Phys. Rev. Lett.* **123**, 180501 (2019).

[27] C. Chen, L. Jin, and R.-B. Liu, Sensitivity of parameter estimation near the exceptional point of a non-Hermitian system, *New J. Phys.* **21**, 083002 (2019).

[28] Q. Zhong, J. Ren, M. Khajavikhan, D. Christodoulides, S. Ozdemir, and R. El-Ganainy, Sensing with exceptional surfaces in order to combine sensitivity with robustness, *Phys. Rev. Lett.* **122**, 153902 (2019).

[29] H. Wang, Y.-H. Lai, Z. Yuan, M.-G. Suh, and K. Vahala, Petermann-factor sensitivity limit near an exceptional point in a Brillouin ring laser gyroscope, *Nat. Commun.* **11**, 1610 (2020).

[30] R. Duggan, S. A. Mann, and A. Alù, Limitations of sensing at an exceptional point, *ACS Photonics* **9**, 1554 (2022).

[31] W. Ding, X. Wang, and S. Chen, Fundamental sensitivity limits for non-Hermitian quantum sensors, *Phys. Rev. Lett.* **131**, 160801 (2023).

[32] J. Naikoo, R. W. Chhajlany, and J. Kołodyński, Multiparameter estimation perspective on non-Hermitian singularity-enhanced sensing, *Phys. Rev. Lett.* **131**, 220801 (2023).

[33] H. Loughlin and V. Sudhir, Exceptional-point sensors offer no fundamental signal-to-noise ratio enhancement, *Phys. Rev. Lett.* **132**, 243601 (2024).

[34] J. H. Rivero, L. Feng, and L. Ge, Imaginary gauge transformation in momentum space and Dirac exceptional point, *Phys. Rev. Lett.* **129**, 243901 (2022).

[35] Y. Wu, D. Zhu, Y. Wang, X. Rong, and J. Du, Experimental observation of Dirac exceptional points, *Phys. Rev. Lett.* **134**, 153601 (2025).

[36] A. H. Castro Neto, F. Guinea, N. M. R. Peres, K. S. Novoselov, and A. K. Geim, The electronic properties of graphene, *Rev. Mod. Phys.* **81**, 109 (2009).

[37] K. S. Novoselov, A. K. Geim, S. V. Morozov, D. Jiang, M. I. Katsnelson, I. V. Grigorieva, S. V. Dubonos, and A. A. Firsov, Two-dimensional gas of massless Dirac fermions in graphene, *Nature* **438**, 197 (2005).

[38] X.-J. Yu, Z. Pan, L. Xu, and Z.-X. Li, Non-Hermitian strongly interacting Dirac fermions, *Phys. Rev. Lett.* **132**, 116503 (2024).

[39] Z. Wang, Y. Sun, X.-Q. Chen, C. Franchini, G. Xu, H. Weng, X. Dai, and Z. Fang, Dirac semimetal and topological phase transitions in  $A_3Bi$  ( $A=Na, K, Rb$ ), *Phys. Rev. B* **85**, 195320 (2012).

[40] Z. K. Liu, B. Zhou, Y. Zhang, Z. J. Wang, H. M. Weng, D. Prabhakaran, S.-K. Mo, Z. X. Shen, Z. Fang, X. Dai, Z. Hussain, and Y. L. Chen, Discovery of a three-dimensional topological Dirac semimetal,  $Na_3Bi$ , *Science* **343**, 864 (2014).

[41] M. Neupane, S.-Y. Xu, R. Sankar, N. Alidoust, G. Bian, C. Liu, I. Belopolski, T.-R. Chang, H.-T. Jeng, H. Lin, A. Bansil, F. Chou, and M. Z. Hasan, Observation of a three-dimensional topological Dirac semimetal phase in high-mobility  $Cd_3As_2$ , *Nature Commun.* **5**, 3786 (2014).

[42] N. P. Armitage, E. J. Mele, and A. Vishwanath, Weyl and Dirac semimetals in three-dimensional solids, *Rev. Mod. Phys.* **90**, 015001 (2018).

[43] X. Wan, A. M. Turner, A. Vishwanath, and S. Y. Savrasov, Topological semimetal and Fermi-arc surface states in the electronic structure of pyrochlore iridates, *Phys. Rev. B* **83**, 205101 (2011).

[44] S.-Y. Xu, I. Belopolski, N. Alidoust, M. Neupane,

G. Bian, C. Zhang, R. Sankar, G. Chang, Z. Yuan, C.-C. Lee, S.-M. Huang, H. Zheng, J. Ma, D. S. Sanchez, B. Wang, A. Bansil, F. Chou, P. P. Shibayev, H. Lin, and M. Z. Hasan, Discovery of a Weyl fermion semimetal and topological Fermi arcs, *Science* **349**, 613 (2015).

[45] T. Meng and J. C. Budich, Unpaired Weyl nodes from long-ranged interactions: Fate of quantum anomalies, *Phys. Rev. Lett.* **122**, 046402 (2019).

[46] Y.-C. Tzeng and M.-F. Yang, Fate of Fermi-arc states in gapped Weyl semimetals under long-range interactions, *Phys. Rev. B* **102**, 035148 (2020).

[47] A. Banerjee and A. Narayan, Non-Hermitian semi-Dirac semi-metals, *J. Phys.: Cond. Mat.* **33**, 225401 (2021).

[48] D.-J. Zhang, Q.-h. Wang, and J. Gong, Quantum geometric tensor in  $\mathcal{PT}$ -symmetric quantum mechanics, *Phys. Rev. A* **99**, 042104 (2019).

[49] D. D. Solnyshkov, C. Leblanc, L. Bessonart, A. Nalitov, J. Ren, Q. Liao, F. Li, and G. Malpuech, Quantum metric and wave packets at exceptional points in non-Hermitian systems, *Phys. Rev. B* **103**, 125302 (2021).

[50] J.-F. Ren, J. Li, H.-T. Ding, and D.-W. Zhang, Identifying non-Hermitian critical points with the quantum metric, *Phys. Rev. A* **110**, 052203 (2024).

[51] Y.-C. Tzeng, C.-Y. Ju, G.-Y. Chen, and W.-M. Huang, Hunting for the non-Hermitian exceptional points with fidelity susceptibility, *Phys. Rev. Res.* **3**, 013015 (2021).

[52] Y.-T. Tu, I. Jang, P.-Y. Chang, and Y.-C. Tzeng, General properties of fidelity in non-Hermitian quantum systems with PT symmetry, *Quantum* **7**, 960 (2023).

[53] Y.-M. R. Hu, E. A. Ostrovskaya, and E. Estrecho, Generalized quantum geometric tensor in a non-Hermitian exciton-polariton system [invited], *Opt. Mater. Express* **14**, 664 (2024).

[54] C.-Y. Ju, A. Miranowicz, F. Minganti, C.-T. Chan, G.-Y. Chen, and F. Nori, Einstein's quantum elevator: Hermitianization of non-Hermitian Hamiltonians via the Vielbein formalism, *Phys. Rev. Res.* **4**, 023070 (2022).

[55] Y. Wu, W. Liu, J. Geng, X. Song, X. Ye, C.-K. Duan, X. Rong, and J. Du, Observation of parity-time symmetry breaking in a single-spin system, *Science* **364**, 878 (2019).

[56] W. Zhang, X. Ouyang, X. Huang, X. Wang, H. Zhang, Y. Yu, X. Chang, Y. Liu, D.-L. Deng, and L.-M. Duan, Observation of non-Hermitian topology with nonunitary dynamics of solid-state spins, *Phys. Rev. Lett.* **127**, 090501 (2021).

[57] C.-Y. Ju, A. Miranowicz, G.-Y. Chen, and F. Nori, Non-Hermitian Hamiltonians and no-go theorems in quantum information, *Phys. Rev. A* **100**, 062118 (2019).

[58] D.-J. Zhang, Q.-h. Wang, and J. Gong, Time-dependent  $\mathcal{PT}$ -symmetric quantum mechanics in generic non-Hermitian systems, *Phys. Rev. A* **100**, 062121 (2019).

[59] V. Meden, L. Grunwald, and D. M. Kennes,  $\mathcal{PT}$ -symmetric, non-Hermitian quantum many-body physics—a methodological perspective, *Rep. Prog. Phys.* **86**, 124501 (2023).

[60] C.-Y. Ju, A. Miranowicz, Y.-N. Chen, G.-Y. Chen, and F. Nori, Emergent parallel transport and curvature in Hermitian and non-Hermitian quantum mechanics, *Quantum* **8**, 1277 (2024).

[61] B. Gardas, S. Deffner, and A. Saxena, Non-Hermitian quantum thermodynamics, *Sci. Rep.* **6**, 23408 (2016).

[62] C.-Y. Ju, A. Miranowicz, J. Barnett, G.-Y. Chen, and F. Nori, Heisenberg and Heisenberg-like representations via Hilbert-space-bundle geometry in the non-Hermitian regime, *Phys. Rev. A* **111**, 052213 (2025).

[63] W.-M. Chen, Y.-T. Lin, and C.-Y. Ju, Non-Hermitian generalization of Rayleigh-Schrödinger perturbation theory, *Phys. Rev. A* **111**, 022211 (2025).

[64] R. Jozsa, Fidelity for mixed quantum states, *J. Mod. Opt.* **41**, 2315 (1994).

[65] W.-L. You, Y.-W. Li, and S.-J. Gu, Fidelity, dynamic structure factor, and susceptibility in critical phenomena, *Phys. Rev. E* **76**, 022101 (2007).

[66] M.-F. Yang, Ground-state fidelity in one-dimensional gapless models, *Phys. Rev. B* **76**, 180403(R) (2007).

[67] Y.-C. Tzeng and M.-F. Yang, Scaling properties of fidelity in the spin-1 anisotropic model, *Phys. Rev. A* **77**, 012311 (2008).

[68] Y.-C. Tzeng, H.-H. Hung, Y.-C. Chen, and M.-F. Yang, Fidelity approach to Gaussian transitions, *Phys. Rev. A* **77**, 062321 (2008).

[69] S.-J. Gu, Fidelity approach to quantum phase transitions, *Int. J. Mod. Phys. B* **24**, 4371 (2010).

[70] X.-J. Yu, S. Yang, J.-B. Xu, and L. Xu, Fidelity susceptibility as a diagnostic of the commensurate-incommensurate transition: A revisit of the programmable Rydberg chain, *Phys. Rev. B* **106**, 165124 (2022).

[71] H. Jiang, C. Yang, and S. Chen, Topological invariants and phase diagrams for one-dimensional two-band non-Hermitian systems without chiral symmetry, *Phys. Rev. A* **98**, 052116 (2018).

[72] N. Matsumoto, K. Kawabata, Y. Ashida, S. Furukawa, and M. Ueda, Continuous phase transition without gap closing in non-Hermitian quantum many-body systems, *Phys. Rev. Lett.* **125**, 260601 (2020).

[73] Y. Nishiyama, Fidelity-susceptibility analysis of the honeycomb-lattice Ising antiferromagnet under the imaginary magnetic field, *Eur. Phys. J. B* **93**, 1 (2020).

[74] G. Sun, J.-C. Tang, and S.-P. Kou, Biorthogonal quantum criticality in non-Hermitian many-body systems, *Frontiers of Physics* **17**, 33502 (2022).

[75] W.-Y. Zhang, M.-Y. Mao, Q.-M. Hu, X. Zhao, G. Sun, and W.-L. You, Yang-Lee edge singularity and quantum criticality in non-Hermitian PXP model, *Phys. Rev. B* **112**, 155135 (2025).

[76] C.-Y. Ju and F.-H. Huang, Quantum state evolution and Berry potentials at exceptional points and quantum phase transitions, *New J. Phys.* **27**, 124505 (2025).

[77] T. Kato, *Perturbation theory for linear operators*, 2nd ed., Grundlehren der mathematischen Wissenschaften (Springer, Berlin, 1976).